

# Microfluidic based single cell microinjection

Andrea Adamo and Klavs F. Jensen

Received 25th February 2008, Accepted 16th June 2008

First published as an Advance Article on the web 1st July 2008

DOI: 10.1039/b803212b

**We report a microfluidic based approach for single cell microinjection in which fluid streams direct a cell onto a fixed microneedle in contrast to moving a microneedle towards an immobilized cell, as done in conventional methods. The approach simplifies microinjection and offers the potential for flow through automated microinjection of cells.**

Delivery of molecules across the cell membrane is an important step in many experimental biological protocols, such as those involved in RNA interference<sup>1</sup> and the generation of transgenic animals.<sup>2</sup> The increasing need for efficient intracellular delivery of macromolecules into living cells has fostered the development of a variety of techniques, which can be grouped into three classes: chemical methods (synthetic vectors), biological methods (viral vectors) and physical methods.<sup>3</sup> Chemical approaches are widely used and rely on the self assembly of a liposome around the molecules to be delivered. The formed liposome then shuttles the enclosed macromolecules into the cell. Chemical methods are relatively cheap and effective, but they suffer from not being quantitative, to some extent toxic, and not efficient in a variety of conditions.<sup>4</sup> Biological methods exploit the ability of viral organism to deliver their cargo into living cells. Viral vectors are efficient in terms of delivery rate, but they are expensive, limited in breadth of applications, occasionally toxic and not quantitative (*i.e.*, it is not possible to determine how many molecules are delivered into each cell).<sup>5,6</sup> The third class of intracellular delivery methods, physical approaches,<sup>7</sup> involves a wide variety of techniques physically opening holes in the cell membrane, including microinjection,<sup>8</sup> electroporation,<sup>9</sup> and ultrasound treatments.<sup>10</sup> Among these methods, microinjection stands out as the only existing technique that allows efficient introduction of a wide variety of molecules (*e.g.*, lipids, proteins, drugs, *etc.*) or structures (*e.g.* sub-cellular organelles or nanofabricated structures) in a quantitative fashion into single cells. Unfortunately, traditional microinjection techniques are costly and time consuming.<sup>11</sup>

At present, microinjection is performed with expensive equipment consisting of a microscope for cell visualization and robotic arms for cell manipulation. Using the robotic arm, a trained operator holds a single cell in place with a pipette and pierces it with a pulled glass microneedle. The compound of interest is injected through the microneedle and the cell is released. An experienced operator can typically inject up to 100 cells

per hour. This slow delivery rate renders microinjection a non viable approach for many biological applications and limits it to specific low throughput operations such as *in vitro* fertilization.<sup>12</sup> Increases in injection throughput (~1000 cells per hour) have been achieved with a recent automated microinjector<sup>13</sup> in which cell immobilization is achieved by a microfluidic sieve and the microinjection is subsequently performed by a robot positioning the micro needle successively on each cell.

Herein, we describe a disposable microfluidic device for low cost, quantitative microinjection in which the usual microinjection strategy is reversed. Cell injection is achieved by moving cells onto a stationary microneedle instead of moving the needle into an immobilized cell. In the operation of the device (Fig. 1), a suspended cell coming from a supply reservoir is first lined up in the micro channel (channel A) and then transported towards the needle by the fluidic stream draining through Channel C with Channel B closed (Fig. 1.1). The two actuation valves, V1 and V2, are pneumatic valves that obstruct Channels C and B, respectively, by deformation of a thin elastomeric membrane under the action of pressurized air.<sup>14</sup> Once the cell is pierced by the needle, the injection is performed (Fig. 1.2). Channel C is then closed and channel B opened (Fig. 1.3). The main flow with the help of the backpressure and backflow generated by the actuation of valve V1 lifts the cell off the needle and carries the injected cell to a collection reservoir. The system can now be reset to the condition of frame 1 and be ready to inject the next cell. The pressure drops across channel B and C are designed to be equal so that there is no overall significant change of flow rate upon valve actuation.

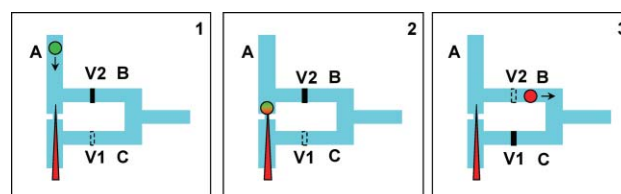


**Fig. 1** Schematic representation of the microfluidics based single cells microinjection system. 1: Cell to be injected is moved by the fluid stream towards a fixed microneedle, valve 1 (V1) is open while valve 2 (V2) is closed. 2: The cell impinges on the needle and is pierced. Microinjection is performed (turning the cell from green to red). 3: V2 is open and V1 is closed causing the fluid stream and the volume displaced by valve V1 operation to lift the cell off the needle and carry it through channel B towards a collection reservoir.

Dept. of Chemical Engineering, Massachusetts Institute of Technology, 77 Massachusetts Ave., Cambridge, MA, 02139, USA.  
E-mail: aadam@mit.edu; Fax: +1 617 258 8992; Tel: +1 617 253 1929, kjensen@mit.edu; Fax: +1 617 258 8992; Tel: +1 617 253 4589

The microfluidic cell injection system (Fig. 2) was realized in polydimethylsiloxane (PDMS, Sylgard 184, Dow Corning, USA) by soft lithography.<sup>15</sup> Chrome masks were generated by

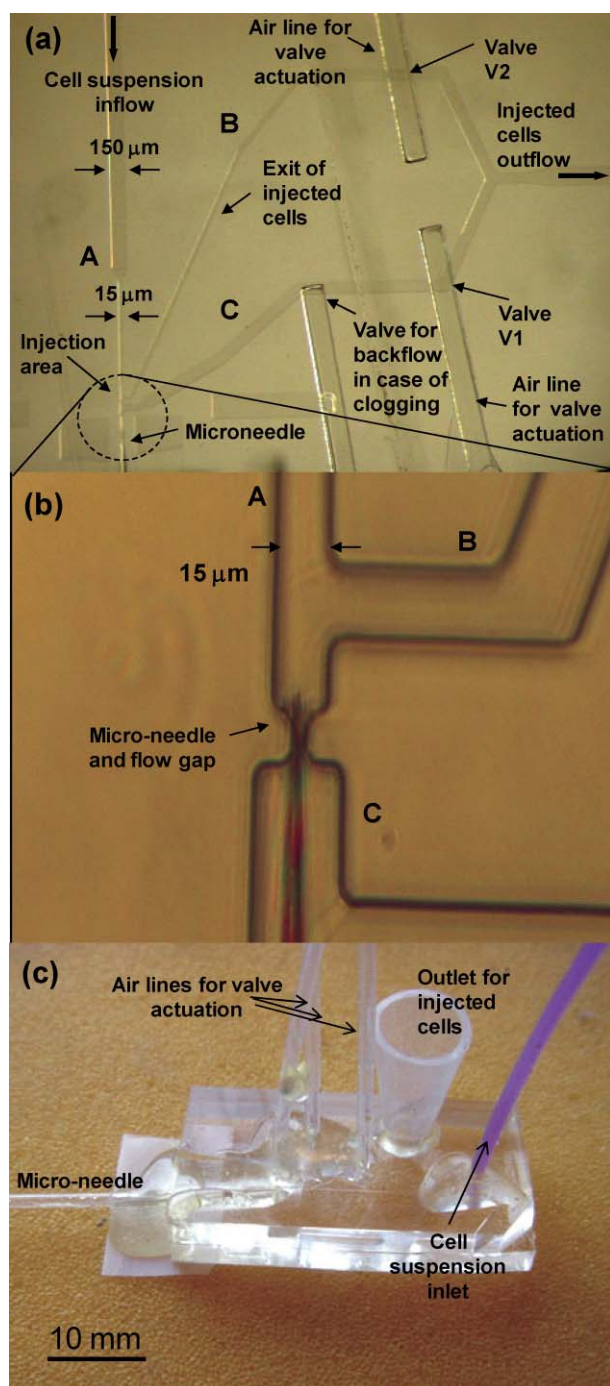


**Fig. 2** (a) Microscopy image of the microinjection chip. Channels A, B, and C as well as valves, V1 and V2, correspond to those labelled in Fig. 1. Additionally, the figure shows a valve to release a “cell-jam” as described in the text. (b) Microscopy image of the injection area. (c) Assembled microinjection device.

laser direct writing (Heidelberg Instruments, Heidelberg, Germany) and these were used to pattern SU8-2015 (Microchem Corp., Newton, MA, USA) masters.

In order to position the cell in front of the needle and ultimately pierce the cell membrane, the injection area and the channel A were designed with dimensions similar to those of the cells used for the experiments (15  $\mu\text{m}$  in diameter and 15  $\mu\text{m}$  in height). For the injection portion, the gap separating the

injection chamber from channel C was designed to be small enough to prevent cell bypass of the needle while allowing fluid flow around the needle. Experiments showed that a gap of 5  $\mu\text{m}$  in width and 5  $\mu\text{m}$  in length produced the necessary cell blocking with a reasonable pressure drop.

The pneumatic valves<sup>14</sup> were microfabricated by a two step fabrication process. In a first step, the microfluidic channels used to move the cells were formed by spin coating a 100  $\mu\text{m}$  thick PDMS layer onto a SU8 master supported on a silicon wafer. After curing (5 min at 100  $^{\circ}\text{C}$ ), a second thin layer ( $\sim 80$   $\mu\text{m}$ ) of PDMS was spun onto the wafer to act as a “glue” to attached this unit to a second PDMS slab ( $\sim 500$   $\mu\text{m}$  thick) carrying the air lines for the actuation of the valves. The air lines were 200  $\mu\text{m}$  wide by 100  $\mu\text{m}$  deep and were formed by SU8 based soft-lithography analogous to the microfluidic channel layer. Both the sets of channels had rectangular cross-sections. A final baking cured the “glue” layer fixing the air channel layer above the microfluidic channel layer.

The patterned PDMS were peeled off the supporting SU8-silicon wafer master and soaked in triethylamine, ethyl acetate and acetone (for 2 hours for each solvent; all solvents were analytical grade, triethylamine, Sigma–Aldrich, USA; acetone, Mallinckrod, USA; ethyl acetate, EM Science–Merck, USA). The solvent wash was performed to reduce cell adhesion to the channel walls and to make the PDMS surface characteristics more reproducible.<sup>16</sup> Finally, the microfluidic channels were sealed by bonding the PDMS chip to a PDMS slab ( $\sim 4$  mm thick) with a 30 s air plasma treatment (PDC-32G, Harrick Scientific) to activate both surfaces.

For piercing and injecting cells, we used commercial microinjection needles made of pulled glass capillaries with tip internal diameter of 0.5  $\mu\text{m}$  (World Precision Instruments, Sarasota, USA). The glass capillary was inserted into the cell handling chip *via* an access trench cut into the chip with a surgical blade following alignment marks. A 3D micro stage and a stereomicroscope enabled the insertion and precise positioning of the needle inside the chip. With the chip fixed, the needle was moved with the 3D micro stage and positioned into the chip. The capillary was guided down the above described trench until the tip of the needle entered the bottom of channel A. The needle location was then adjusted by fine movements of the microstage to achieve a protrusion of the glass microcapillary into channel A of 2–5  $\mu\text{m}$ . This fine positioning was critical to avoid impaling the cell completely (*i.e.* piercing of the cells all the way through).

Because of the different refractive indexes of air and PDMS, the first step of moving the needle in channel A required tilting of the board with the chip and the micro stages so that the cross section of the bottom of channel A could be clearly seen through the trench. Visual guidance by the aid of the stereo microscope allowed positioning of the needle tip inside the channel A. At that point, the board with chip and micropositioners was tilted back to the horizontal position and the final protrusion of the needle into channel A was finely adjusted by viewing the glass capillary through the PDMS. Illumination from below enhanced the success rate of the needle placement procedure. Finally, the needle was secured to the chip with epoxy (Devcon 5 min epoxy).

We first tested the ability to generate reversible fluidic streams by using fluorescent micro beads and optimized the hydraulic features of the device. Valves showed good seals with pressure in

the air lines of  $\sim 1.5$  bar. Next, HeLa cells cultured in Dulbecco modified eagle medium (DMEM) with 10% fetal calf serum, and penicillin ( $10 \text{ units ml}^{-1}$ ) and streptomycin ( $10 \mu\text{g ml}^{-1}$ ) were used to explore if transit of the cells through the microinjection chip (without performing cell piercing and injection) had any significant effect on cell viability. After detachment with trypsin and re-suspension in phosphate buffered solution without calcium or magnesium (PBS), cells were flown into the chip ( $4\text{--}40 \text{ nl min}^{-1}$ ) or maintained in a sterile tube adjacent to the chip for control. Viability analysis by Trypan Blue staining showed no differences in cell viability between the two conditions with 98% cell viability one hour after passage through the chip.

After having demonstrated the ability to manipulate beads and that flowing cells did not adversely affect the cells, we then proceeded to test the microinjection of HeLa cells. Cell speeds in the range  $0.3\text{--}3 \text{ mm s}^{-1}$  (corresponding flow rates in the present device of  $4\text{--}40 \text{ nl min}^{-1}$ ) were adequate to impart enough momentum to the cell to achieve piercing by the needle without clogging the channel by squeezing the cell in the narrow gap that provides communication between channel A and C (Fig. 1). Injection was performed with constant flow through the needle. The injected volume was controlled by varying the time the cell spent positioned on the needle. In this proof of concept device, injection flow and cell time on the needle were controlled by the operator using visual observation with an inverted microscope. Setting the flow rate through the microneedle to  $0.02 \mu\text{l h}^{-1}$  with a syringe pump (Cole Palmer EW-74900-10, USA), cells were injected with  $\sim 2.5 \text{ pL}$  while positioned on the needle for about  $0.5 \text{ s}$ .

During the testing and optimization phase we rarely observed clogging of the needle due to cell impact. More frequently, clogging of channel A occurred due by the presence very large cells or by non specific adhesion of cells to the channel walls. Large cells were excluded by introducing a fork structure at the chip inlet to prevent entrance of oversized cells. Cell adhesion was mitigated by the solvent cleaning of the PDMS (described above). In order to further reduce cell clogging, we added a second valve in channel C to provide backflow in the case of a “cell-jam”.

In order to visualize the injection of material into cells, we selected a fluorescent marker compound, dextran, tetramethylrhodamine MW 10 000 (Molecular probes, USA), which is unable to cross cell membranes—except when microinjected.<sup>17</sup> HeLa cells were pierced and successfully injected with the dextran (Fig. 3). Cell injection was successfully performed multiple times. Viability of injected cells was assessed first by the absence of cell coloration in the presence of Trypan Blue and then by culturing of the injected cells (Fig. 4). The injected cells were viable 24 hours after the injection as assessed by adherence on tissue culture plastic and morphology analysis.

In summary, we have designed, microfabricated and tested a device for microfluidic based microinjection into living cells. The device is based on a new concept in which cells are moved onto a fixed needle by fluid streams. The current proof of concept device and experimental set-up allow only injection of a few cells with the device in one experimental session. Nonetheless, the microfluidic approach, when compared to existing microinjection approaches, potentially allows higher throughputs and lower costs. Injection of a cell and removal of

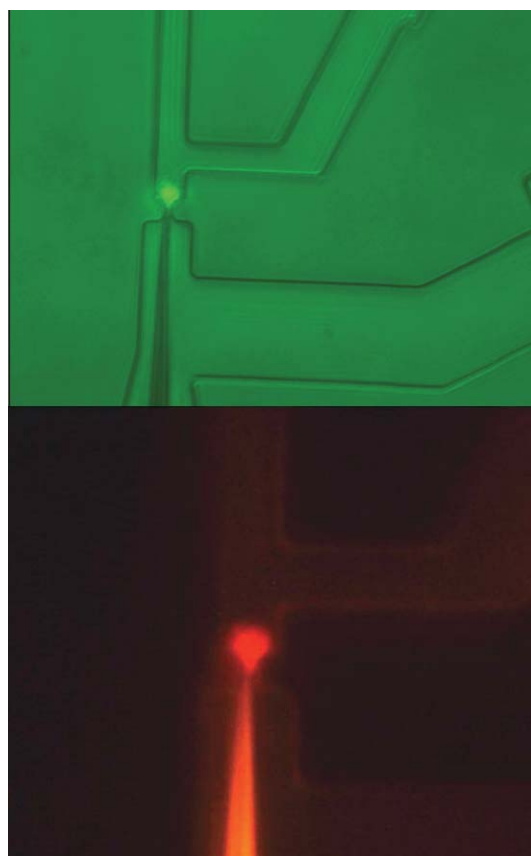


**Fig. 3** Top: image of cell pierced by the needle (the cell is dyed with vital dye, Acridine orange). Bottom: image of cell being injected with dextran—the red fluorescent dextran conjugate is observed in both the needle and in the cell.

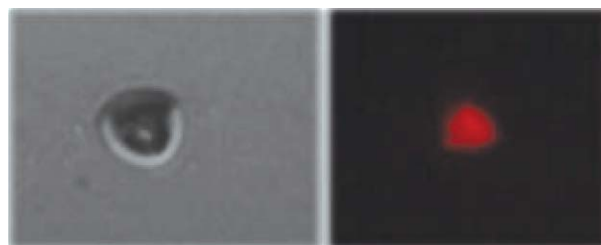


**Fig. 4** Left: a bright field picture of an injected cell in the culture. Right: the same cell with a red fluorescence from the injected dextran conjugate.

the injected cell from the injection chambers typically takes less than a  $1/10$  second with an average residence time in the chip of about  $5 \text{ min}$  (chip internal volume  $\sim 60 \text{ nl}$ ). Therefore, as a rough conservative estimate, with adequate concentration of the cell suspension, it is reasonable to expect that an automated system would be able to perform at least one cell injection per second corresponding to an injection rate of  $\sim 3600 \text{ cell h}^{-1}$ . Moreover, the microfabricated device combines soft lithography defined microfluidics with conventional glass capillary microneedles. This use of inexpensive and disposable parts offers the potential for production of disposable microinjection devices that eliminate problems and costs related to cleaning and maintenance of conventional microinjection equipment.

---

## Acknowledgements

The work was supported in part by the National Institutes of Health (P50-GM68762).

## Notes and references

- 1 I. R. Gilmore, S. P. Fox, A. J. Hollins and S. Akhtar, *Curr. Drug Delivery*, 2006, **2**, 147.
- 2 L. Tesson, J. Cozzi, S. Ménoret, S. Rémy, C. Usal, A. Fraichard and I. Aneon, *Transgenic Res.*, 2005, **5**, 531.
- 3 X. Gao, K. S. Kim and D. Liu, *AAPS J.*, 2007, **9**, E92.
- 4 D. Liu, E. F. Chiao and H. Tian, *Methods Mol. Biol.*, 2004, **245**, 3.
- 5 J. T. Douglas, *Methods Mol. Biol.*, 2004, **246**, 3.
- 6 N. Somia, *Methods Mol. Biol.*, 2004, **246**, 463.
- 7 T. H. Chou, S. Biswas and S. Lu, *Methods Mol. Biol.*, 2004, **245**, 147.
- 8 T. E. Wagner, P. C. Hoppe, J. D. Jollick, D. R. Scholl, R. L. Hodinka and J. B. Gault, *Proc. Natl. Acad. Sci. U. S. A.*, 1981, **10**, 6376.
- 9 J. Gehl, *Acta Physiol. Scand.*, 2003, **4**, 437.
- 10 B. D. Meijering, R. H. Henning, W. H. Van Gilst, I. Gavrilovic, A. Van Wamel and L. E. Deelman, *J. Drug Targeting*, 2007, **10**, 664.
- 11 R. King, *Methods Mol. Biol.*, 2004, **245**, 167.
- 12 W. Heuwieser, X. Yang, S. Jiang and R. H. Foote, *Mol. Reprod. Dev.*, 1992, **4**, 489.
- 13 [http://www.computers.us.fujitsu.com/downloads/biosciences/14.WP\\_cellinjector\\_0306.pdf](http://www.computers.us.fujitsu.com/downloads/biosciences/14.WP_cellinjector_0306.pdf), 2006.
- 14 Marc A. Unger, Hou-Pu Chou, Todd Thorsen, Axel Scherer and Stephen R. Quake, *Science*, 2000, **288**, 113.
- 15 Younan Xia and George m. Whitesides, *Annu. Rev. Mater. Sci.*, 1998, **28**, 153–84.
- 16 Jonathan Vickers, Meghan M. Caulum and Charles Henry, *Anal. Chem.*, 2006, **78**, 7446.
- 17 A. Bevilacqua, R. Loch-Carusio and R P. Erickson, *Proc. Natl. Acad. Sci. U. S. A.*, 1989, **14**, 5444.